Chemical Engineering Journal 101 (2004) 251–260

Chemical Engineering Journal

www.elsevier.com/locate/cej

Generation of metal nanoparticles in a microchannel reactor

J. Wagner [a,*], T. Kirner [a], G. Mayer [b], J. Albert [b], J.M. Köhler [a,b]

[a] *Physical Chemistry and Microreaction Technology Department, Institute of Physics, Technical University of Ilmenau, Germany*

[b] *Institute for Physical High Technology, Jena, Germany*

Abstract

Twelve nanometer Au nanoparticles generated by citrate reduction were handled in a chip-based interdiffusion microreactor without significant adsorption to the surfaces at flow rates in the μl/min-range. Furthermore, the microreactor was tested for the generation and growth of colloidal gold nanoparticles. Following a seeding growth approach, starting from 12 nm citrate-stabilised gold seeds, larger particles of diameters ranging from 15 to 24 nm were prepared. This method makes use of ascorbic acid as reducing agent, while the 12 nm seeds serve as nucleation centers. For particle stabilization polyvinyl pyrrolidone was employed. Particle size distributions were determined by an analytical centrifugation method or atomic force microscopy. UV-Vis spectra of the colloidal solutions were recorded. The size distribution of the produced particles is altered by the flow rate of the reactants, their concentration ratio as well as the order of the reactant addition. In the conducted experiments the mean particle diameter increases with decreasing flow rate and particle growth was only observed, if the concentration of seeds was equal or lower than the concentration of Au^{3+}. Without the addition of polyvinyl pyrrolidone, the produced colloidal solutions were unstable and decomposed within 7 days.

Keywords: Polyvinyl pyrrolidone; Ascorbic acid; Colloidal solutions; Gold nanoparticles; Chip reactor

1. Introduction

Within the last years the research on the synthesis and modification of nanoparticles has an increasing impact on materials and surface science. Colloidal metal particles show great potential for catalysis [1,2] as well as for analytical applications such as surface enhanced Raman spectroscopy [3], colorimetric gene detection [4], nanoparticle-enhanced microchip capillary electrophoresis [5] and optical detection of specific molecular interactions [6,7]. Thus, the synthesis and properties of such particles have attracted considerable scientific and commercial interest and different classes of substances and particles are under investigation, e.g. organic particles [8], micellar systems [9], metal and semiconductor particles [10], oxidic particles [11] as well as complex particles [12].

Another fast growing field of research and scientific interest is microreaction technology. Within the last decade a multitude of components was developed for a variety of microfluidic, microchemical, analytical, sensor, biochemical and molecular biological applications [13–17].

Hence we combined both technologies and handled as well as synthesised nanoparticles in microsystems. But there are difficulties accompanying the handling of heterogeneous systems in microreactors, such as adhesion, transport behaviour and particle adsorption. Thus there are only a few papers that deal with particles in microchannels, namely with regard to particle manipulation [18] and the development of solid phase syntheses [19]. Recently other groups have started working on particle synthesis in microreactors as well, and so inorganic salt nanocrystallites [20–23] and semiconductor (CdSe) nanoparticles [24] have been synthesised in a microsystem set-up. However, to the best of our knowledge no results have been published about metal nanoparticles synthesised in microreactors yet. Hence, this contribution is the first report about a microsystem set-up for the generation of gold nanoparticles in a continuous flow system.

2. Experimental

2.1. Materials

Trisodium citrate dihydrate (Merck, Germany), chloroauric acid trihydrate (Roth, Germany), ascorbic acid (Merck, Germany), polyvinyl pyrrolidone (polyvidone, PVP) (Merck, Germany) were used as received. Deionised water

* Corresponding author. Tel.: +49-3677-69-32-32; fax: +49-3677-69-31-79.
E-mail address: joerg.wagner@tu-ilmenau.de (J. Wagner).

1385-8947/$ – see front matter © 2003 Elsevier B.V. All rights reserved.
doi:10.1016/j.cej.2003.11.021

(Aqua purificator G 7795, Miele, Germany) was used for all preparations. All solutions were passed through a 0.2 μm syringe filter (Whatmann, USA) before use, to remove particles larger than 200 nm.

2.2. Instrumentation

Particle sizing studies of the Au nanoparticles were performed using an analytical centrifugation system (DC 20000, CPS Instruments Inc., USA), which yields directly the particle size distribution of the liquid sample. For determination of morphology of the particles as well we used an atomic force microscopy (AFM) facility at the IPHT, Jena (Dimension 3100 microscope, Digital Instruments, USA). For these studies the samples were prepared on a (thoroughly cleaned) microscope slide. Electronic absorption spectra were recorded using a two beam UV-Vis spectrometer (Specord 200, Analytik Jena AG, Germany). All experiments were performed in a clean room to avoid cross contamination and at room temperature, i.e. at 22 °C, as controlled by air condition. Microscopic pictures of the channels inside the microreactor were taken using a video microscope (Motic DM 143, Motic B1 series, Motic Deutschland GmbH, Germany) and an image processing software (Motic Images 2000, release 1.2, Motic Deutschland GmbH, Germany).

2.3. Microsystem set-up (Fig. 1)

Microsystem set-up is shown in Fig. 1. The microchannel reactor, which was produced at IPHT Jena, is designed as outlined in Fig. 2. The channels are wet etched in Pyrex glass and covered with a layer of silicon, which is anodic bonded to the glass. The reactor possesses two residence zones and four microfluidic ports (A–D), that are etched into the silicon. Three of these ports served as inlets and one as outlet. The reactor with a volume of 2.3 μl, was embedded in a microfluidic environment, whose components were connected via flexible PTFE tube (inner diameter: 0.3 mm). Syringe pumps (SP210iw, World Precision Instruments Inc., USA or 540210, TSE Technical & Equipment GmbH, Germany) equipped with 1.0 ml polypropylene syringes (“Omnifix”, Roth, Germany) were used for filling the reactor with reagent solutions. In this way low continuous flow rates in the order of 10 μl/min could be achieved.

2.4. Preparation of 12 nm Au particles (seeds)

Hayat in “Colloidal Gold—Principles, Methods and Applications”, describes the method used for these particles [25]. Briefly, 1.75 ml trisodium citrate ($Na_3C_6H_6O_7$) solution ($c = 40.8$ mM) was added to 50 ml of a boiling solution of chloroauric acid ($c = 0.3$ mM) in a beaker while stirring. On addition the solution turned red within a few minutes. The colloidal solution was cooled to room temperature and stored at 4 °C. Before further utilization of these nanoparticles, the solution was passed through a 0.2 μm syringe filter to remove greater aggregates, which might have developed during storage. To control the quality of the colloidal solution, both UV-Vis analysis and analytical centrifugation method were performed, yielding a single absorption band with $\lambda_{max} = 518$ nm and a mean particle diameter of 11.7 nm ± 0.9 nm.

2.5. Adsorption tests

Twelve nanometer Au particles were passed through the reactor (inlet A to outlet D, see Fig. 2) at pH = 10 and at different flow rates (50, 25, 10 and 5 μl/min). The solutions were collected in polypropylene centrifuge tubes and analysed immediately after the test to compare the characteristics of the solution with the ones measured before passing the reactor. The UV-Vis absorption and the particle diameter distribution were measured before and after the passage. Furthermore microscopic photographs of the microchannels were taken to control possible fouling.

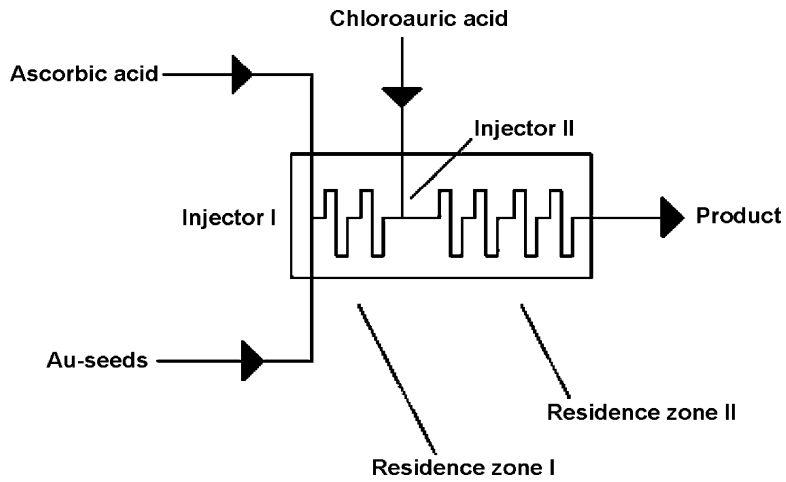

Fig. 1. Schematic drawing of the experimental set-up and the connectivity of the reactor in Experiments II–V.

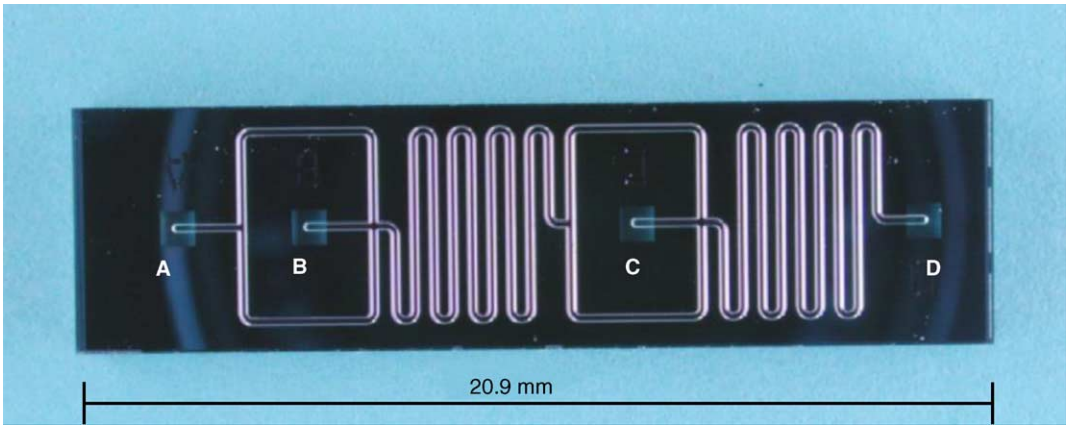

Fig. 2. Photograph of the microchannel reactor designed and produced by IPHT Jena.

2.6. Preparation of Au nanoparticles in the presence of seed

Following a method suggested by Jana et al. [26] 12 nm Au particles served as seeds for the generation of larger particles within the channels of the microreactor. The three inlets (A, B and C, see Fig. 2) were used to pump solutions of 12 nm Au seeds (inlet A), ascorbic acid (B or C) and chloroauric acid (C or B) at different flow rates through the reactor, where they mix due to diffusion within the small channels. The flow rates and the concentration of the reagents (and hence their concentration ratio) as well as the order of their addition differ from experiment to experiment. But in all experiments the fore-runnings, i.e. in Experiment I 12 nm Au seeds + ascorbic acid and in all other experiments 12 nm Au seeds + $HAuCl_4$, were also collected for comparison. In detail the experimental conditions can be depicted as follows:

- *Experiment I*: 12 nm Au seeds (0.30 mM, A), chloroauric acid (0.25 mM, B) and ascorbic acid (60 mM, C) at 25 μl/min each.
- *Experiment II*: 12 nm Au seeds (0.30 mM, A), chloroauric acid (1.0 mM, C) and ascorbic acid (24 mM, B) at 50 μl/min each.
- *Experiment III*: 12 nm Au seeds (0.30 mM, A), chloroauric acid (1.0 mM, C) and ascorbic acid (24 mM, B) at 25 μl/min each.
- *Experiment IV*: 12 nm Au seeds (0.30 mM, A), chloroauric acid (1.0 mM, C) and ascorbic acid (24 mM, B) at 10 μl/min each.
- *Experiment V*: 12 nm Au seeds (0.30 mM, A), chloroauric acid (0.08 mM, C) and ascorbic acid (24 mM, B) at 25 μl/min each.

After collection, the solutions were checked for changes in UV-Vis absorption and size distribution, as well as for their pH values which were always between 5 and 6. Additionally in Experiments II–V the solutions were divided into two volumina (each 900 μl), one of these staying unchanged and the other mixed with 10 μl of PVP solution (5% w/v), to stabilize the gold nanoparticles. In Experiment II both product solutions were checked for changes after 7 days of storage.

3. Results

3.1. Adsorption tests

At a flow rate of 50 μl/min the UV-Vis spectra of both solutions are congruent (Fig. 3). That means that the optical density and the spectral characteristics of the solution are unaffected through contact with the reactor surfaces, meaning that the concentration and electronic properties of the Au particles stay the same, at this flow rate. The analysis of the particle size distribution is shown in Fig. 4 and again one can observe no difference between the curves, i.e. the particle size distribution is not altered while the particles flow through the reactor at 50 μl/min. Even at lower flow rates (25, 10 and 5 μl/min) the adsorption is very low as shown by the marginal change in the UV-Vis spectra for the adsorption experiment at 5 μl/min (Fig. 3). The absorption at λ_{max} decreases about 3.4%, corresponding to a reduction in nanoparticle concentration in the same order. For 25 and 10 μl/min the absorption is reduced by 5.3 and 2.5%, respectively. Furthermore, incubation of the microreactor with nanoparticle solution over night did not lead to visible contamination of the microchannel with gold, as shown by Fig. 5.

3.2. Nanoparticle growth

It was shown that greater nanoparticles can be synthesised by growing 12 nm gold seeds in the microchannel reactor. All synthesised colloidal solutions have been investigated by UV-Vis spectroscopy. For particle size determination either analytical centrifugation (CPS system) or AFM were applied. The results clearly prove that there is an increase in particle size if 12 nm Au seeds, $HAuCl_4$ solution and

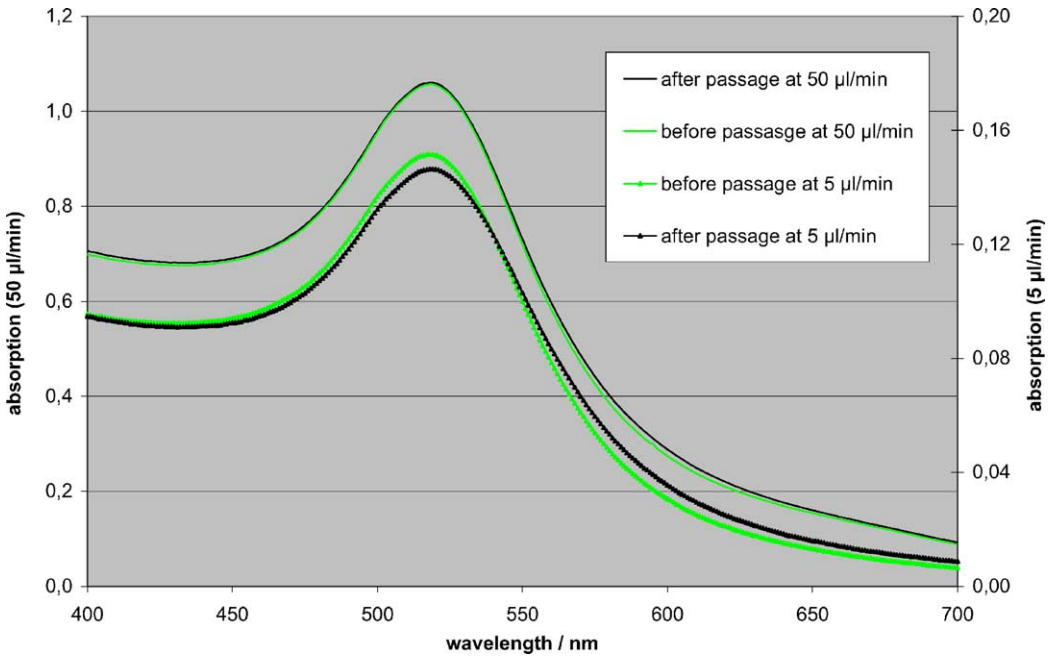

Fig. 3. UV-Vis spectra of 12 nm Au particle solutions before and after passing the interdiffusion microreactor at 50 and 5 μl/min, respectively.

ascorbic acid (acting as reducing agent) are mixed in the interdiffusion reactor. Several experiments were employed using different concentration ratios of the reactants as well as different flow rates. For example, in Experiment I chloroauric acid, 12 nm Au seeds and ascorbic acid were used at a concentration ratio of 1/1.25/250. All solutions were pumped through the reactor at 25 μl/min yielding a product solution with the following characteristics. The particle size increases significantly (Fig. 6b) as compared to the solution pumped through the reactor without ascorbic acid (Fig. 6a). This could be due to agglomeration or particle growth. Furthermore, there is a broadening of the particle size distribution and a dilution of observable particles (Fig. 6), latter probably caused by the ascorbic acid addition which dilutes the particle solution. The diameters determined by measuring 20 particles in the AFM picture are 12.2 nm (±3.2 nm) for the seeds and 23.7 nm (±9.2 nm) for the grown particles. The size distribution change is also detectable in the

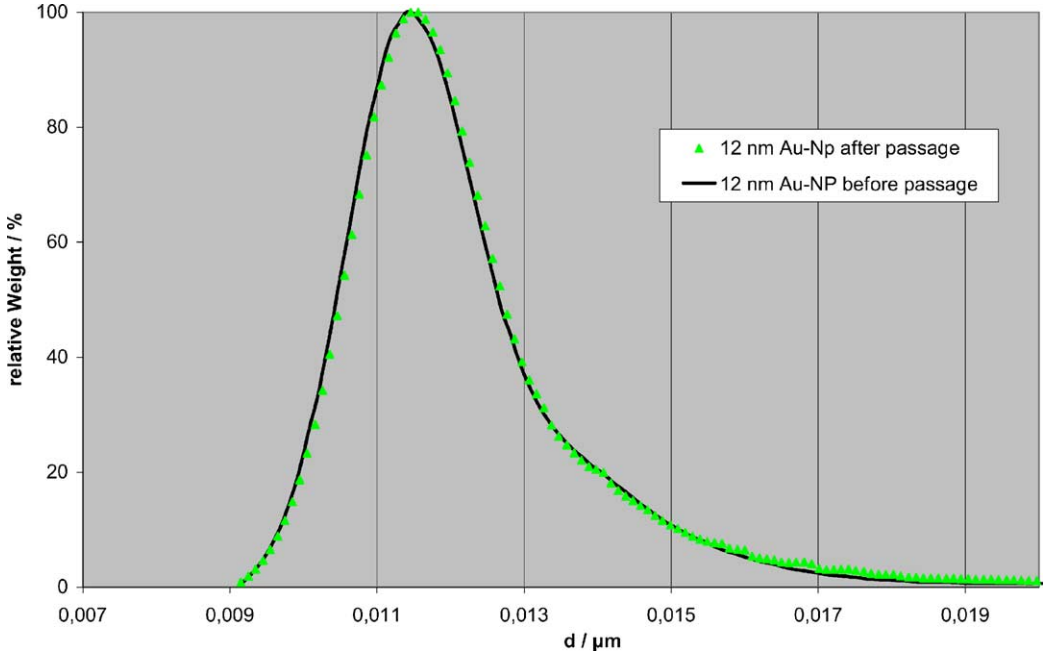

Fig. 4. CPS analysis of 12 nm Au particle solution before and after passing the interdiffusion microreactor at 50 μl/min.

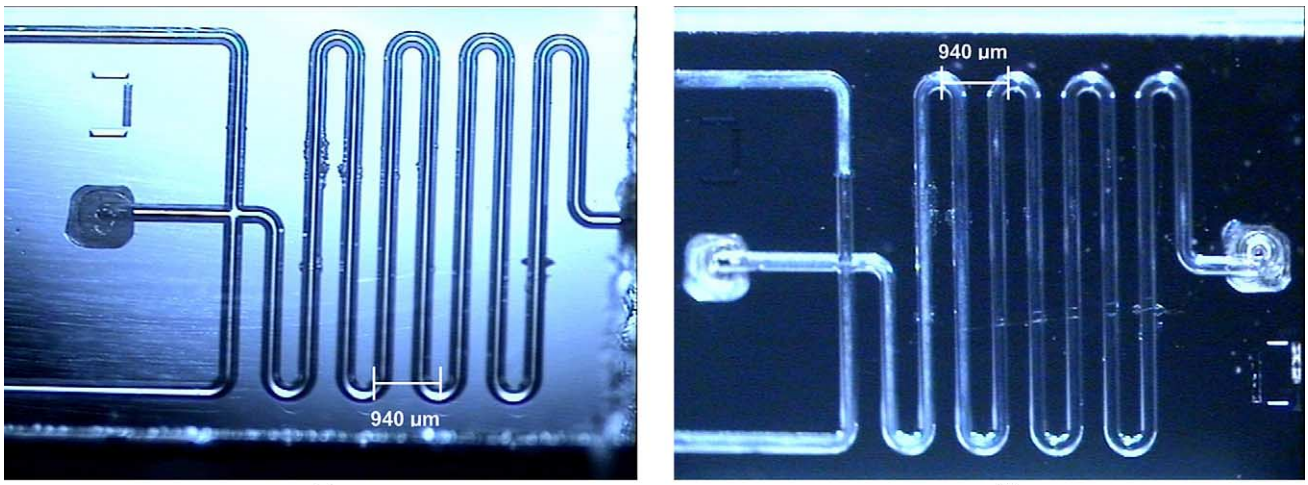

Fig. 5. (a) Microscopic photograph of the microreactor before; (b) microscopic photograph of the microreactor after 20 h incubation with 12 nm Au nanoparticle solution of incubation with 12 nm Au nanoparticle solution.

absorption spectrum (Fig. 7). The absorption peak maximum for 12 nm Au seeds is at 525 nm ($A = 0.85$), while it is at 533 nm ($A = 0.96$) for grown particles, whose spectrum also shows a stronger absorption in the longer wavelength region>600 nm. In Experiment II the concentration ratio of 12 nm Au seeds to chloroauric acid was 1/3 at a flow rate of 50 μl/min each and the seeds were mixed with ascorbic acid first, while $HAuCl_4$ was the third reactant. Furthermore, the product solutions were divided into two volumina (each 900 μl), one of these staying unchanged and the other mixed with 10 μl of PVP solution (5% w/v), which is known for stabilising gold nanoparticles The results shown in Figs. 8 and 9 indicate the change in particle size distribution achieved by this experiment. Again, the absorption peak maximum is bathochromic "red" shifted for the product solution (product: $\lambda_{max} = 535$ nm; product + PVP: $\lambda_{max} = 533$ nm; 12 nm seeds mixed with chloroauric acid, called fore-runnings: $\lambda_{max} = 520$ nm). Here the particle sizing was done using the CPS-system and yields the following values—product: 15.4 nm (±5.3 nm); product + PVP: 13.2 nm (±3.4 nm); 12 nm seeds mixed with chloroauric acid ("fore-runnings"): 11.8 nm (±2.2 nm). The analysis for both product solution was repeated after a week, showing that the non-stabilised particles agglomerate, leading to a clear solution and a black sediment, while the solution containing PVP shows still the same UV-Vis spectrum ($\lambda_{max} =$

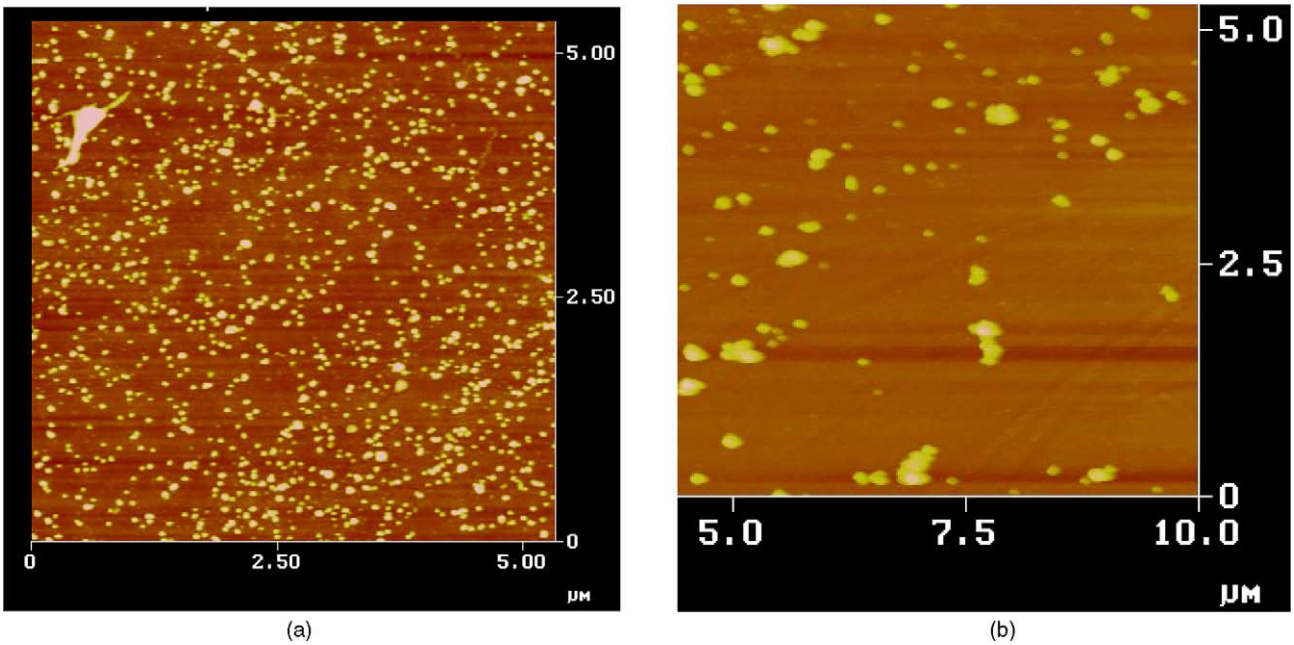

Fig. 6. (a) AFM image of 12 nm Au seeds on a microscope slide; (b) AFM image of Au particles grown from 12 nm seeds in Experiment I.

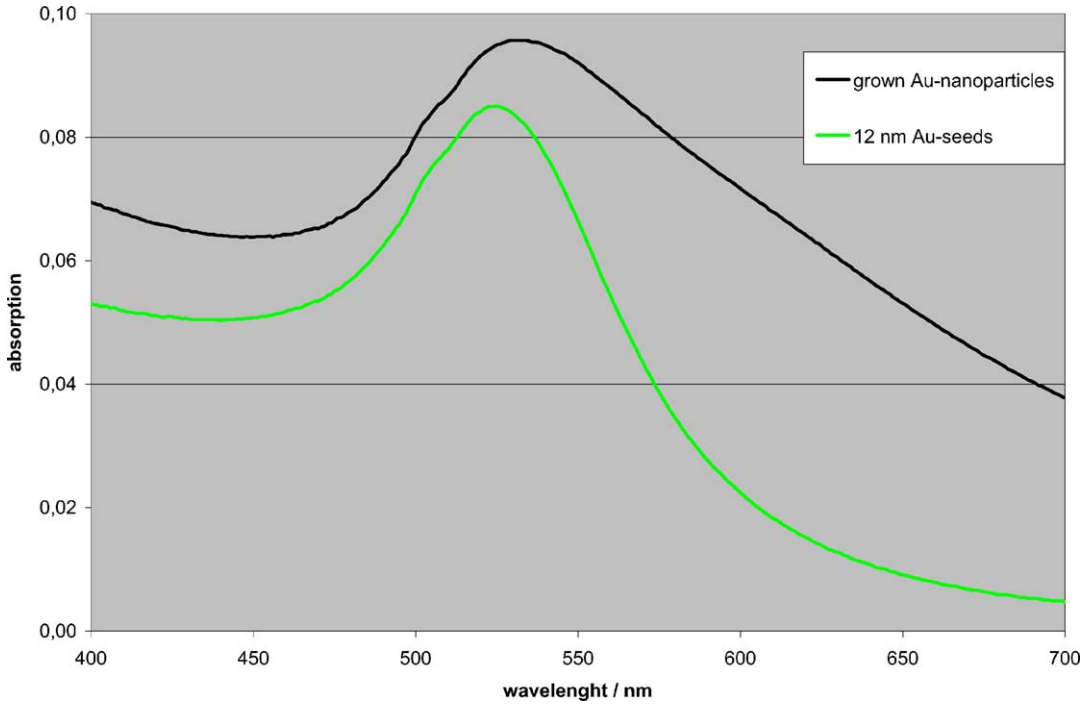

Fig. 7. UV-Vis spectra of initial 12 nm Au seeds and enlarged particles in Experiment I.

533 nm) and mean particle diameter (13.4 nm). Several more experiments were conducted, e.g. Experiment III at 25 μl/min and Experiment IV at 10 μl/min as well as Experiment V, where an inversed concentration ratio of 12 nm Au seeds and chloroauric acid, i.e. 3/1, was used. The results of these reactions are summarised in Table 1, together with the results described above. At 10 μl/min a significant precipitation of gold in the microchannels occurred (Fig. 10) and further experiments at lower flow rates were not performed.

4. Discussion

4.1. Adsorption tests

One of the most important issues for manipulation of micro- and nanoparticles is their adsorption to the surfaces, that are very large in proportion to the volume of the reactor. Adsorbed particles cannot take part in the reaction as the ones dispersed and would be detained from transport.

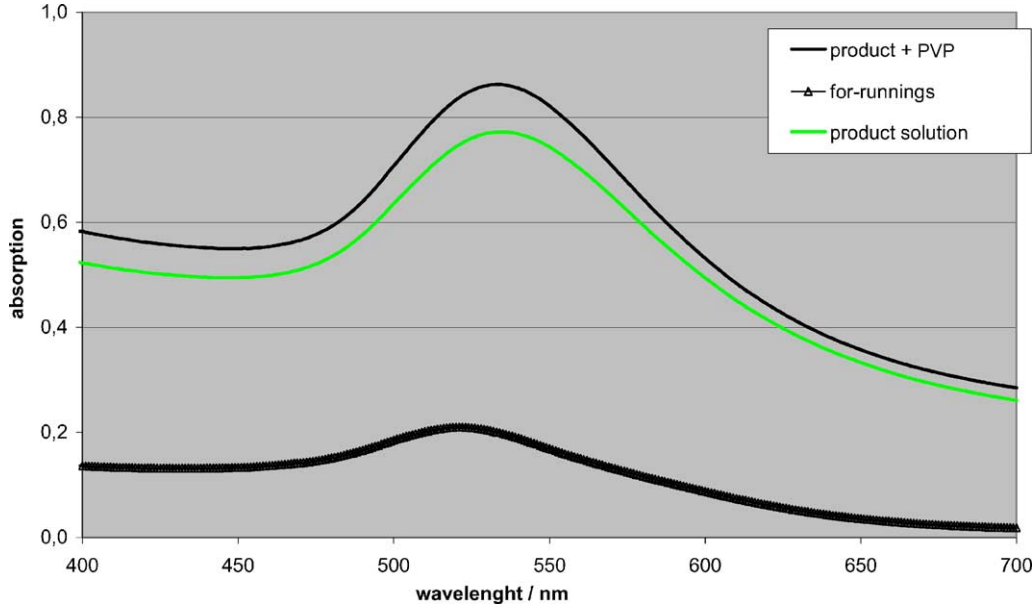

Fig. 8. UV-Vis spectra of fore-runnings (12 nm Au seeds + ascorbic acid) and product solutions in Experiment II.

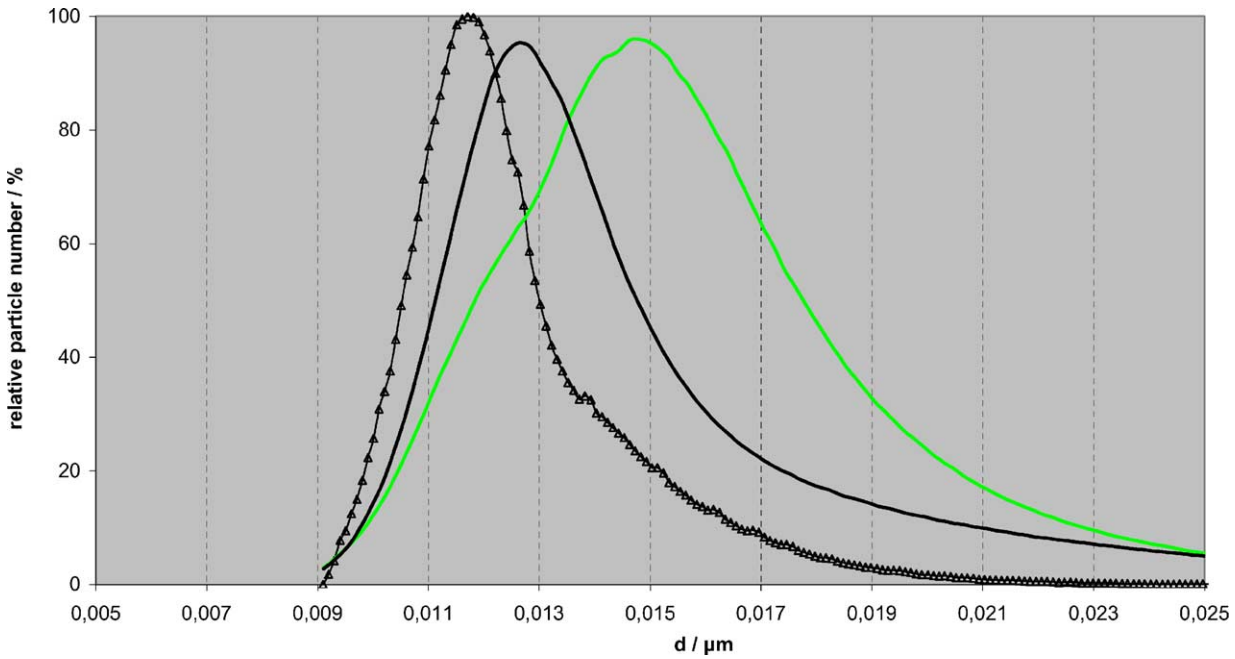

Fig. 9. Size distribution (CPS analysis) of fore-runnings (12 nm Au seeds + ascorbic acid) and product solutions in Experiment II: (△) fore-runnings; (grey straight line) product; (black straight line) product + PVP.

Particles can stick to the reactor surfaces by chemical or physical sorption, determining the kind of interaction which leads to adsorption. Either way, the aim is to avoid any kind of adsorption to assure the transport of all substances, i.e. nanoparticles, through the reactor and inhibit "fouling" of the microchannels. The surface of native silicon and glass, of which the reactors are made of, is hydrophilic. It consists of SiO_2 and Si–OH groups [27], whose density is considered to be 5×10^{14} OH groups/cm^2 [28]. Depending on the pH value of the fluid inside the reactor and the pK_a of the surface OH groups (between 4 and 9) [29] these groups can also occur as deprotonated Si–O$^-$ groups. This property can be used by adjusting the pH of the nanoparticle solution to 10, which leads to a complete deprotonation of the surface Si–OH groups and hence to negative net charge on the surface. Provided the citrate-stabilised particles do have a negative charge at the surface, which they certainly have at this pH, the particles repel from the surface by electrostatic repulsion.

The results of the particle adsorption experiments prove this behaviour. The absorption of the nanoparticle solution in the UV-Vis spectra and hence the nanoparticle concentration

Table 1
Experimental conditions and characteristics of the produced colloidal solutions in the conducted experiments

Experiment	Flow rate (μl/min)	Concentration ratio (seeds/Au^{3+})	Product fraction	UV-Vis		Diameter, d (nm)	Deviation[a]		Sizing method
				λ_{max} (nm)	A (cm)		σ (nm)	σ (%)	
I	25	1:1.25	Fore-runnings	525	0.85	12.2	3.2	26.2	AFM
			Product	533	0.86	23.7	9.2	38.8	AFM
II	50	1:3	Fore-runnings	520	0.21	11.9	1.1	9.2	CPS
			Product	535	0.77	15.4	2.7	17.5	CPS
			Product + PVP	533	0.86	13.2	1.7	12.9	CPS
III	25	1:3	Fore-runnings	520	0.24	12.7	1.7	13.4	CPS
			Product	537	0.75	17.8	3.2	18.0	CPS
			Product + PVP	529	0.47	13.2	2.0	15.2	CPS
IV	10	1:3	Fore-runnings	519	0.23	12.2	1.3	10.7	CPS
			Product	531	0.55	18.7	3.1	16.6	CPS
			Product + PVP	526	0.45	12.2	1.7	13.9	CPS
V	25	3:1	Fore-runnings	519	0.25	12.5	1.3	10.4	CPS
			Product	517	0.27	11.8	1.4	11.9	CPS
			Product + PVP	519	0.28	11.5	1.1	9.6	CPS

[a] In case of CPS sizing σ was calculated from the half width (HW) of the size distribution using the following expression: $\sigma = \mathrm{HW}/(2 \times \ln 2)^{1/2}$.

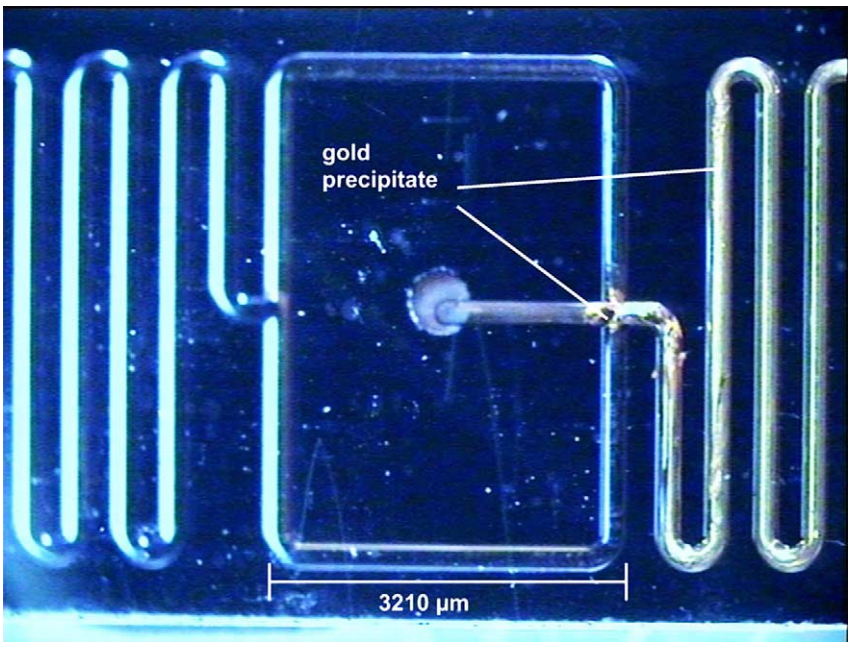

Fig. 10. Microscopic photograph of the microreactor after synthesis at 10 μl/min (the gold deposition is clearly visible in the second residence zone).

stays the same by passing the reactor at 50 μl/min. For smaller flow rates, adsorption of gold particles becomes evident as one can see by the loss of absorption of the solutions after passage. But even in the worst case, the reduction amounts only to 5%. Additionally incubation of the reactor with the nanoparticle solution over night did not lead to visible contamination of the microchannels Fig. 5a and b). So the adsorption behaviour is acceptable for our purposes, because no blocking of the reactor occurs. The adsorption of some nanoparticles does not interfere with the seed-mediated particle growth method, since gold particles are present as nucleation centers in the reaction mixture by definition.

4.2. Seeding growth approach

In nanoparticle synthesis the frequently assumed general mechanistic steps are nucleation and growth stages, both being ideally separated in time to obtain a narrow size distribution of the produced particles. In the reduction reaction of metal salts to metallic nanoparticles, the species at the early stages of the reaction, namely metal atoms and clusters have short lifetimes and are highly reactive. Their redox potential is a function of the cluster size. Due to this size-dependent redox property, the chemical reduction of a metal salt frequently strongly depends on solution conditions as well as on the layout of the reaction vessel [26]. Often difficulties in controlling the nucleation and growth steps of particle formation lead to a wide particle size distribution. A common approach to overcome these difficulties, involved in nanoparticle synthesis, is the use of seeding growth methods. In these methods small particles, which are prepared separately serve as nucleation centers (seeds) for the generation of greater particles. Providing a certain (and controlled) seed concentration and reaction conditions that inhibit secondary nucleation the particle size could be controlled simply by varying the ratio of seed concentration to metal salt concentration. However, those conditions are hard to find, which leads to limited applicability of this method. Generally suitable conditions include a reducing agent too weak to reduce the metal salt (directly) in the absence of seed. Unfortunately it was often observed that the presence of seed rather results in further nucleation than particle growth, when the ratio of seed to metal was relatively small, resulting in a broad size distribution [30].

4.3. Seeds

In this work 12 nm Au seeds were prepared separately following a classical route suggested by Hayat [25], resulting in a colloidal solution with a relatively narrow size distribution ($\sigma \leq 15\%$), as determined by CPS analysis. These particles were used as seeds in a particle growth reaction that took place in a microchannel reactor.

4.4. Particle growth

The results, as given in Table 1, prove that it is possible to transfer the seed-mediated nanoparticle synthesis method to a microsystem set-up. In Experiments I–IV, the particle size distribution of the product solutions is significantly altered compared to the seed size distribution. The mean diameter increases but also the width of the size distribution becomes larger (Table 1). The most obvious enlargement of the particles was observed in Experiment I. The much wider particle

size distribution obtained in this experiment compared to the others is due to the different sizing method. Here the colloidal solution cannot be considered to be monodisperse, since the standard deviations found by evaluation of AFM data are too large ($\sigma \leq 15\%$). However, this sample was also examined using CPS which yielded a standard deviation of approximately 14%. Hence, it is presumed that AFM measurements leads to higher standard deviations. But it is to say that almost all other obtained particle solutions are monodisperse, even those of the enlarged particles, i.e. the product solutions, do not show standard deviations greater than 18%.

4.5. Influence of flow rates

From the performed experiments it is evident that decreasing flow rates results in an increasing mean diameter of the product particles, while the width of the size distribution stays the same on changing the flow rates. To correlate the flow rate in more detail with the mean particle diameter more experiments using a constant seed/Au^{3+} ratio at varying flow rates need to be conducted.

4.6. Concentration ratio

The results also suggest that the particle growth is most efficient (+11.5 nm at 25 μl/min) in the case where the seed/Au^{3+} ratio is close to unity (Experiment I). For smaller seed/Au^{3+} ratios (Experiment II–IV) there is still particle growth but less efficient (+5.1 nm at 25 μl/min). But this discrepancy could also be due to the different order of reactant addition in Experiment I compared to the other experiments. A high seed/Au^{3+} ratio, which Jana et al. [30] claims to be favourable for suppressing secondary nucleation in favour to particle growth proved not to be applicable under the chosen conditions. In Experiment V, where the seed/Au^{3+} ratio is approximately 3/1 no particle growth is observed, as revealed by the UV-Vis and CPS analysis. Even secondary nucleation seems not to occur, since there is no increase in absorption after the reaction.

4.7. PVP addition

The apparent reduction in mean particle diameter as well as in the width of the size distribution on addition of the polymer PVP is most likely an imaginary one, due to the sizing methods working principle. The CPS system makes use of differences in the sedimentation velocities of particles of different sizes but comparable surface properties and bulk densities in a centrifugational force field. Hence, the coverage of the Au nanoparticle surface with the bulky PVP chains (probably random coiled) results in a change of the nanoparticle properties, that is much more significant as the surface coverage with the relatively small citrate ions, for example. There could be a reduction in the average density of the particle (density of gold $\gg$ density of PVP) and even more probable there is a change in the (fluid) flow resistance of the particle moving through the liquid during sedimentation. Both changes would result in a reduced sedimentation velocity corresponding to detection of particles with smaller diameter and explaining the CPS results. Thus, it is to assume that the product particle solutions containing PVP do not really consist of smaller particles. To reveal the real mean diameter of these particles scanning tunnelling microscope (STM) investigations are currently in progress. However, the PVP addition results in stable properties of the colloidal solutions as documented by UV-Vis and CPS investigations, that where conducted after 1 week storage of the solutions. In contrast the unstabilised solutions decompose, i.e. agglomeration is obvious as the solution becomes clear and colourless while a black precipitate is formed.

5. Conclusion and outlook

It was shown that 12 nm Au nanoparticles can be handled in microchannel reactors without blocking the channels. Furthermore, greater particles were generated using a seeding growth approach. Particle size was altered by adjusting the flow rate of the reactants. The order of addition as well as the concentration ratio of the reactants did also influence the particle size distribution. Addition of the polymer PVP leads to stable colloidal solutions but also to a reduction in mean particle diameter as revealed by CPS analysis, that is not fully understood yet. Currently the particle size distribution of these solutions is under investigation using STM and AFM. Future work will include a closer examination of the influence of reaction parameters as concentration of the reagents and pH on the size and shape of the generated particles. The continuous flow character of the experimental set-up will strongly support these experiments since it offers the opportunity to easily change the reaction parameters homogeneously. In addition the possibility of straightforward nanoparticle synthesis starting directly from the uncomplexed metallic species is currently under investigation. Furthermore, we are working on an extension of the microsystem to alter the surface reactivity of the particles in a second reaction step by attaching molecules to the surface. These functionalised particles shall later be used for labelling experiments and further investigated with respect to their transport behaviour.

Acknowledgements

We would like to thank the cleanroom staff at IPHT Jena for the production of the microreactors. Furthermore we thank F. Möller (TU Ilmenau) for embedding the reactor in the microsystem environment and for assistance with the experiments. This work was funded by German Federal Environmental Foundation (DBU).

References

[1] M. Sastry, P. Mukherjee, C.R. Patra, A. Ghosh, R. Kumar, Chem. Mater. 14 (2002) 1678–1684.
[2] R.M. Crooks, M.Q. Zhao, L. Sun, V. Chechik, L.K. Yeung, Accounts Chem. Res. 34 (2001) 181–190.
[3] A.N. Shipway, E. Katz, I. Willner, Chem. Phys. Chem. 1 (2000) 18–52.
[4] J.M. Köhler, A. Csaki, J. Reichert, R. Möller, W. Straube, W. Fritzsche, Sens. Actuators B 76 (2001) 166–172.
[5] J. Wang, E. Grushka, R. Polsky, M. Pumera, Anal. Chem. 73 (2001) 5625–5628.
[6] A. Henglein, Chem. Mater. 10 (1998) 444–450.
[7] A. Chilkoti, N. Nath, Anal. Chem. 74 (2002) 504–509.
[8] X. Marguerettaz, A. Merrins, D. Fitzmaurice, J. Mater. Chem. 8 (1998) 2157–2164.
[9] M.P. Pileni, Langmuir 13 (1997) 3266–3276.
[10] R.A. Bley, S.M. Kauzlarich, in: J.H. Fendler (Ed.), Nanoparticles and Nanostructured Films, Wiley-VCH, Weinheim, 1998, p. 101.
[11] E.A. Meulenkamp, J. Phys. Chem. B 102 (1998) 5566–5572.
[12] L.M. Bronstein, M. Antonietti, P.M. Valetsky, in: J.H. Fendler (Ed.), Nanoparticles and Nanostructured Films, Wiley-VCH, Weinheim, 1998, p. 145.
[13] W. Ehrfeld, Microreaction Technology: Industrial Prospects, in: W. Ehrfeld (Ed.), Proceedings of the Third International Conference on Microreaction Technology, Springer, Berlin/Heidelberg, 1999.
[14] I. Schneegaß, J.M. Köhler, R. Bräutigam, Lab on a Chip 1 (2001) 42.
[15] O. Wörz, Chemie in unserer Zeit 34 (2000) 24–29.
[16] V. Hessel, H. Löwe, Chemie Ingenieur Technik 74 (2002) 17–30.
[17] V. Hessel, H. Löwe, Chemie Ingenieur Technik 74 (2002) 185–207.
[18] T. Müller, et al., J. Loq. Chrom. Rel. Technoly 23 (2000) 47.
[19] A. Schober, A. Schwienhorst, J.M. Köhler, R. Günther, M. Thürk, Microsyst. Technol. 1 (1995) 168.
[20] N. Jongen, M. Donnet, P. Bowen, J. Lemaitre, H. Hofmann, R. Schenk, Ch. Hofmann, M. Aoun-Habbache, S. Guillemet-Fritsch, J. Sarrias, A. Rousset, M. Viviani, M.T. Buscaglia, V. Buscaglia, P. Nanni, A. Testino, J.R. Herguijuela, Chem. Eng. Technol. 26 (2003) 303–305.
[21] N. Jongen, M. Donnet, P. Bowen, J. Lemaitre, Ch. Hofmann, R. Schenk, H. Hofmann, M. Aoun-Habbache, S. Guillement-Fritsch, J. Sarrias, A. Rousset, M. Viviani, M.T. Buscaglia, V. Buscaglia, P. Nanni, A. Testino, J.R. Herguijuela, Chem. Eng. Trans. 1 (2002) 807–812.
[22] R. Schenk, M. Donnet, V. Hessel, Ch. Hofmann, N. Jongen, H. Löwe, in: Proceedings of the Fifth International Conference on Microreaction Technology, 2001, pp. 489–498.
[23] R. Schenk, V. Hessel, B. Werner, F. Schönfeld, Ch. Hofmann, M. Donnet, N. Jongen, Chem. Eng. Trans. 1 (2002) 909–914.
[24] H. Nakamura, Y. Yamaguchi, M. Miyazaki, M. Uehara, H. Maeda, P. Mulvaney, Chem. Lett. (2002) 1072–1073.
[25] M.A. Hayat, Colloidal Gold—Principles, Methods and Applications, vol. I, Academic Press, San Diego/New York/Berkeley/Boston, 1989.
[26] N.R. Jana, L. Gearheart, C.J. Murphy, Chem. Mater. 13 (2001) 2313–2322.
[27] G.M. Whitesides, Y.-T. Tao, S.R. Wasserman, Langmuir 5 (1989) 1074–1087.
[28] G. Friedbacher, H. Hoffmann, H. Brunner, T. Vallant, U. Mayer, B. Basnar, Langmuir 15 (1999) 1899–1901.
[29] R. Kopelman, X. Zhao, J. Phys. Chem. 100 (1996) 11014–11018.
[30] N.R. Jana, L. Gearheart, C.J. Murphy, Langmuir 17 (2001) 6782–6786.